10

Topology Optimization of Fluid Mechanics Problems

Maatoug Hassine
ESSTH, Sousse University
Tunisia

1. Introduction

Optimal shape design problems in fluid mechanics have wide and valuable applications in aerodynamic and hydrodynamic problems such as the design of car hoods, airplane wings and inlet shapes for jet engines. One of the first studies is found in Pironneau (1974). It is devoted to determine a minimum drag profile submerged in a homogeneous, steady, viscous fluid by using optimal control theories for distributed parameter systems. Next, many shape optimization methods are introduced to determine the design of minimum drag bodies Kim and Kim (1995); Pironneau (1984), diffusers Cabuk and Modi (1992), valves Lund et al. (2002), and airfoils Cliff et al. (1998). The majority of works dealing with optimal design of flow domains fall into the category of shape optimization and are limited to determine the optimal shape of an existing boundary.

It is only recently that topological optimization has been developed and used in fluid design problems. It can be used to design features within the domain allowing new boundaries to be introduced into the design. In this context, Borvall and Petersson Borrvall and Petersson (2003) implemented the relaxed material distribution approach to minimize the power dissipated in Stokes flow. To approximate the no-slip condition along the solid-fluid interface they used a generalized Stokes problem to model fluid flow throughout the domain. Later, this approach was generalized by Guest and Prévast in Guest and Prévost (2006). They treated the material phase as a porous medium where fluid flow is governed by Darcy's law. For impermeable solid material, the no-slip condition is simulated by using a small value for the material permeability to obtain negligible fluid velocities at the nodes of solid elements. The flow regularization is expressed as a system of equations; Stokes flow governs in void elements and Darcy flow governs in solid elements.

In this work, we propose a new topological optimization method. Our approach is based on topological sensitivity analysis Amstutz (2005); Amstuts and Masmoudi (2003); Garreau et al. (2001); Guillaume and Hassine (2007); Guillaume and Sid Idris (2004); Hassine et al. (2007); Hassine and Masmoudi (2004); Masmoudi (2002); Sokolowski and Zochowski (1999). The optimal domain is constructed through the insertion of some obstacles in the initial one. The problem leads to optimize the obstacles location. The main idea is to compute the topological asymptotic expansion of a cost function j with respect to the insertion of a small obstacle inside the fluid flow domain. The obstacle is modeled as a small hole $\mathcal{O}_{z,\varepsilon}$ around a point z having an homogeneous condition on the boundary $\partial\mathcal{O}_{z,\varepsilon}$. The best location z of $\mathcal{O}_{z,\varepsilon}$ is given by the most negative value of a scalar function δj, called the topological gradient.

In practice, this approach leads to a simple, fast and accurate topological optimization algorithm. The final domain is obtained using an iterative process building a sequence of geometries $(\Omega_k)_k$ starting with the initial fluid flow domain $\Omega_0 = \Omega$. Knowing Ω_k, the new domain Ω_{k+1} is obtained by inserting an obstacle $\mathcal{O}_k$ in the domain Ω_k; $\Omega_{k+1} = \Omega_k \backslash \overline{\mathcal{O}_k}$. The location and the shape of $\mathcal{O}_k$ are defined by a level set curve of the topological gradient δj_k

$$\mathcal{O}_k = \{x \in \Omega_k, \text{ such that } \delta j_k(x) \leq c_k\},$$

where c_k is a scalar parameter used to control the size of the inserted obstacle. The function δj_k is the leading term of the variation $j(\Omega_k \backslash \overline{\mathcal{O}_{z,\varepsilon}}) - j(\Omega_k)$.

The chapter is organized as follows. In the next section, we present the topological optimization problem related to the Stokes system. The aim is to determine the fluid flow domain minimizing a given cost function. To solve this optimization problem we will use the topological sensitivity analysis method described in the Section 3. It consists in studying the variation of a cost function j with respect to a topology modification of the domain. The most simple way of modifying the topology consists in creating a small hole in the domain. In the case of structural shape optimization, creating a hole means simply removing some material. In the case of fluid dynamics where the domain represents the fluid, creating a hole means inserting a small obstacle $\mathcal{O}$. The topological sensitivity tools which have been developed by several authors Garreau et al. (2001); Schumacher (1995); Sokolowski and Zochowski (1999) allow to find the place where creating a small hole will bring the best improvement of the cost function. The main theoretical results are described in Sections 3.2 and 3.3. In section 3.2, we derive an asymptotic expansion for an arbitrary cost function with respect to the insertion of a small obstacle inside the fluid flow domain. In section 3.3, we derive an asymptotic expansion for two standard examples of cost functions.

As application of the proposed topological optimization method, we consider in Section 4 some engineering applications commonly found in the fluid mechanics literature. In Section 4.1, we present the optimization algorithm. In Section 4.2, we treat the shape optimization of pipes in a cavity. The aim is to determine the optimal shape of the pipes that connect the inlet to the outlets of the cavity minimizing the dissipated power in the fluid. The optimization of injectors location in an eutrophized lake is discussed in Section 4.3. Section 4.4 concerns the approximation of a wanted flow using a topological perturbation of the domain.

2. Topological optimization problem

Let Ω be a bounded domain of $\mathbb{R}^d$, $d = 2, 3$ with smooth boundary Γ. We consider an incompressible fluid flow in Ω described by the Stokes equations. The velocity field u and the pressure p satisty the system

$$\begin{cases} -\nu \, \Delta u + \nabla p = F & \text{in } \Omega \\ \text{div } u = 0 & \text{in } \Omega \\ u = 0 & \text{on } \Gamma, \end{cases} \tag{1}$$

where ν denotes the kinematic viscosity of the fluid, F is a given body force per unit of mass (gravitational force).

The aim is to determine the optimal geometry of the fluid flow domain minimizing a given design function j:

$$\min_{D \in \mathcal{D}_{ad}} j(D), \text{ such that } |D| \leq V_{desired},$$

where j has the form

$$j(D) = J(u_D),$$

with u_D is the velocity field solution to the Stokes system in D and $\mathcal{D}_{ad}$ is a given set of admissible domains.
Here $|D|$ is the Lebesgue measure of D and $V_{desired}$ denotes the target volume (weight).
To solve this shape optimization problem we shall use the topological sensitivity analysis method. It consists in studying the variation of the objective function J with respect to a small topological perturbation of the domain Ω.

2.1 Stokes equations in the perturbed domain

We denote by $\Omega\backslash\overline{\mathcal{O}_\varepsilon}$ the perturbed domain, obtained by inserting a small obstacle $\mathcal{O}_\varepsilon$ in Ω. We suppose that the obstacle has the form $\mathcal{O}_\varepsilon = x_0 + \varepsilon\mathcal{O}$, where $x_0 \in \Omega$, $\varepsilon > 0$ and $\mathcal{O}$ is a given fixed and bounded domain of $\mathbb{R}^d$, containing the origin, whose boundary $\partial\mathcal{O}$ is connected and piecewise of class $\mathcal{C}^1$.
In $\Omega\backslash\overline{\mathcal{O}_\varepsilon}$, the velocity u_ε and the pressure p_ε are solution to

$$\begin{cases} -\nu\Delta u_\varepsilon + \nabla p_\varepsilon = F & \text{in } \Omega\backslash\overline{\mathcal{O}_\varepsilon} \\ \text{div } u_\varepsilon = 0 & \text{in } \Omega\backslash\overline{\mathcal{O}_\varepsilon} \\ u_\varepsilon = 0 & \text{on } \Gamma \\ u_\varepsilon = 0 & \text{on } \partial\mathcal{O}_\varepsilon. \end{cases} \tag{2}$$

Note that for $\varepsilon = 0$, $\Omega_0 = \Omega$ and $(u_0\,,\, p_0)$ is solution to

$$\begin{cases} -\nu\Delta u_0 + \nabla p_0 = F & \text{in } \Omega, \\ \text{div } u_0 = 0 & \text{in } \Omega, \\ u_0 = 0 & \text{on } \Gamma. \end{cases} \tag{3}$$

2.2 Topological optimization problem

Consider now a design function j of the form

$$j(\Omega\backslash\overline{\mathcal{O}_\varepsilon}) = J_\varepsilon(u_\varepsilon), \tag{4}$$

where J_ε is a given cost function defined on $H^1(\Omega\backslash\overline{\mathcal{O}_\varepsilon})^d$ for $\varepsilon \geq 0$ and u_ε is the velocity field solution to the Stokes system (2).
Our aim is to determine the optimal location of the obstacle $\mathcal{O}_\varepsilon$ in the domain Ω in order to minimize the design function j. Then, the optimization problem we consider is given as follows:

$$\min_{\mathcal{O}_\varepsilon \subset \Omega} j(\Omega\backslash\overline{\mathcal{O}_\varepsilon}). \tag{5}$$

To this end, we will derive in the next section a topological asymptotic expansion of the function j with respect to ε.

3. Topological sensitivity analysis

In this section we consider a topological sensitivity analysis for the Stokes equations. We present a topological asymptotic expansion of a design function j with respect to the insertion of a small obstacle $\mathcal{O}_\varepsilon$ inside the domain Ω. The proposed approach is based on the following general adjoint method.

3.1 General adjoint method

Let $(\mathcal{V}_\varepsilon)_{\varepsilon\geq 0}$ be a family of Hilbert spaces depending on the parameter ε, such that, $\forall\varepsilon \geq 0$ $\mathcal{V}_\varepsilon \hookrightarrow \mathcal{V}_0$. For $\varepsilon \geq 0$, we consider
• $\mathcal{A}_\varepsilon : \mathcal{V}_\varepsilon \times \mathcal{V}_\varepsilon \longrightarrow \mathbb{R}$ a bilinear, continuous and coercive form on $\mathcal{V}_\varepsilon$,
• $l_\varepsilon : \mathcal{V}_\varepsilon \longrightarrow \mathbb{R}$ a linear and continuous form on $\mathcal{V}_\varepsilon$.
For all $\varepsilon \geq 0$, we denote by u_ε the unique solution to the problem

$$\mathcal{A}_\varepsilon(u_\varepsilon, w) = l_\varepsilon(w), \quad \forall w \in \mathcal{V}_\varepsilon. \tag{6}$$

Consider now a cost function of the form $j(\varepsilon) = J_\varepsilon(u_\varepsilon)$, where J_ε is defined on $\mathcal{V}_\varepsilon$ for $\varepsilon \geq 0$ and J_0 is differentiable with respect to u, its derivative being denoted by $DJ_0(u)$.
Our aim is to derive an asymptotic expansion of j with respect to ε. We consider the following assumptions.

Hypothesis 3.1. *There exist a real number $\delta\mathcal{A}$ and a scalar function $f : \mathbb{R}_+ \longrightarrow \mathbb{R}_+$ such that $\forall\, \varepsilon \geq 0$*

$$\mathcal{A}_0(u_0 - u_\varepsilon, v_0) = f(\varepsilon)\delta\mathcal{A} + o(f(\varepsilon)),$$
$$\lim_{\varepsilon\to 0} f(\varepsilon) = 0,$$

where $v_0 \in \mathcal{V}_0$ is the solution to the adjoint problem

$$\mathcal{A}_0(w, v_0) = -DJ_0(u_0)w, \quad \forall w \in \mathcal{V}_0. \tag{7}$$

Hypothesis 3.2. *There exists a real number δJ such that $\forall\, \varepsilon \geq 0$*

$$J_\varepsilon(u_\varepsilon) - J_0(u_0) = DJ_0(u_0)(u_\varepsilon - u_0) + f(\varepsilon)\delta J + o(f(\varepsilon)).$$

Under the assumptions 3.1 and 3.2, we have the following theorem.

Theorem 3.1. *Hassine et al. (2008) If the assumptions 3.1 and 3.2 hold, the function j has the following asymptotic expansion*

$$j(\varepsilon) = j(0) + f(\varepsilon)\Big(\delta\mathcal{A} + \delta J\Big) + o(f(\varepsilon)).$$

3.2 Topological sensitivity for the Stokes problem

In this section, we derive a topological asymptotic expansion for the Stokes equations. In order to apply the adjoint method described in the previous paragraph, first we establish a variational problem associated to the Stokes system. From the weak variational formulation of (2), we deduce that $u_\varepsilon \in \mathcal{V}_\varepsilon$ is solution to

$$\mathcal{A}_\varepsilon(u_\varepsilon, w) = l_\varepsilon(w), \quad \forall w \in \mathcal{V}_\varepsilon,$$

where the functional space $\mathcal{V}_\varepsilon$, the bilinear form $\mathcal{A}_\varepsilon$ and the linear form l_ε are defined by

$$\mathcal{V}_\varepsilon = \Big\{ w \in H^1_0(\Omega_\varepsilon),\ \mathrm{div}\, w = 0 \ \text{ in } \Omega_\varepsilon \Big\}, \tag{8}$$

$$\mathcal{A}_\varepsilon(v, w) = \nu \int_{\Omega_\varepsilon} \nabla v \cdot \nabla w \,\mathrm{dx}, \quad \forall u, v \in \mathcal{V}_\varepsilon, \tag{9}$$

$$l_\varepsilon(w) = \int_{\Omega_\varepsilon} F\, w \,\mathrm{dx}, \quad \forall w \in \mathcal{V}_\varepsilon, \tag{10}$$

where $\Omega_\varepsilon = \Omega \backslash \overline{\mathcal{O}_\varepsilon}$.
Next we have to distinguish the cases $d = 2$ and $d = 3$, because the fundamental solutions to the Stokes equations in $\mathbb{R}^2$ and $\mathbb{R}^3$ have an essentially different asymptotic behaviour at infinity.

3.2.1 The three dimensional case

Let (U, P) denote a solution to

$$\begin{cases} -\nu \Delta U + \nabla P = 0 & \text{in } \mathbb{R}^3 \backslash \overline{\mathcal{O}} \\ \operatorname{div} U = 0 & \text{in } \mathbb{R}^3 \backslash \overline{\mathcal{O}} \\ U \longrightarrow 0 & \text{at } \infty \\ U = -u_0(x_0) & \text{on } \partial \mathcal{O}. \end{cases} \tag{11}$$

The existence of (U, P) is most easily established by representing it as a single layer potential on $\partial \mathcal{O}$ (see Dautray and Lions (1987))

$$U(y) = \int_{\partial \mathcal{O}} E(y - x) \eta(x) \, \mathrm{ds}(x), \;\; P(y) = \int_{\partial \mathcal{O}} \Pi(y - x) \eta(x) \, \mathrm{ds}(x), \; y \in \mathbb{R}^3 \backslash \overline{\mathcal{O}}$$

where (E, Π) is the fundamental solution of the Stokes equations

$$E(y) = \frac{1}{8\pi\nu r} \left(I + e_r e_r^T \right), \quad \Pi(y) = \frac{y}{4\pi r^3},$$

with $r = ||y||$, $e_r = y/r$ and e_r^T is the transposed vector of e_r. The function $\eta \in H^{-1/2}(\partial \mathcal{O})^3$ is the solution to the boundary integral equation,

$$\int_{\partial \mathcal{O}} E(y - x) \, \eta(x) \, \mathrm{ds}(x) = -u_0(x_0), \; \forall y \in \partial \mathcal{O}. \tag{12}$$

One can observe that the function η is determined up to a function proportional to the normal, hence it is unique in $H^{-1/2}(\partial \mathcal{O})^3 / \mathbb{R} n$.
We start the derivation of the topological asymptotic expansion with the following estimate of the $H^1(\Omega_\varepsilon)$ norm of $u_\varepsilon(x) - u_0(x) - U(x/\varepsilon)$. This estimate plays a crucial role in the derivation of our topological asymptotic expansion. It describes the velocity perturbation caused by the presence of the small obstacle $\mathcal{O}_\varepsilon$.

Proposition 3.1. *Guillaume and Hassine (2007); Hassine et al. (2008) There exists $c > 0$, independent on ε, such that for all $\varepsilon > 0$ we have*

$$\|u_\varepsilon(x) - u_0(x) - U(x/\varepsilon)\|_{1,\Omega_\varepsilon} \leq c\,\varepsilon.$$

The following corollary follows from Proposition 3.1. It gives the behaviour of the velocity u_ε when inserting an obstacle. The principal term of this perturbation is given by the function U, solution to (11).

Corollary 3.1. *We have*

$$u_\varepsilon(x) = u_0(x) + U(x/\varepsilon) + O(\varepsilon), \quad x \in \Omega_\varepsilon.$$

We are now ready to derive the topological asymptotic expansion of the cost function j. It consists in computing the variation $j(\Omega \backslash \overline{\mathcal{O}_\varepsilon}) - j(\Omega)$ when inserting a small obstacle inside the domain. The leading term of this variation involves the function η, the solution to the boundary integral equation (12). The main result is described by Theorem 3.2.

Theorem 3.2. *Guillaume and Hassine (2007); Hassine et al. (2008) If Hypothesis 3.1 holds, the function j has the following asymptotic expansion*

$$j(\Omega\backslash\overline{\mathcal{O}_\varepsilon}) = j(\Omega) + \varepsilon\,\delta j(x_0) + o(\varepsilon).$$

where the topological gradient δj is given by

$$\delta j(x) = \Big(-\int_{\partial\mathcal{O}} \eta(y)\,ds(y)\Big)\cdot v_0(x) + \delta J(x),\ \ x\in\Omega.$$

If $\mathcal{O}$ is the unit ball centred at the origin, $\mathcal{O} = B(0,1)$, the density η is given explicitly $\eta(y) = -\dfrac{3\nu}{2}u_0(x_0)$, $\forall y \in \partial\mathcal{O}$.

Corollary 3.2. *If $\mathcal{O} = B(0,1)$, under the hypotheses of theorem 3.2, we have*

$$j(\Omega\backslash\overline{\mathcal{O}_\varepsilon}) = j(\Omega) + \varepsilon\left[6\pi\nu\, u_0(x_0)\cdot v_0(x_0) + \delta J(x_0)\right] + o(\varepsilon).$$

3.2.2 The two dimensional case

In this paragraph, we present the topological asymptotic expansion for the Stokes equations in the two dimensional case. The result is obtained using the same technique described in the previous paragraph. The unique difference comes from the expression of the fundamental solution of the Stokes equations. In this case (E, Π) is given by

$$E(y) = \frac{1}{4\pi\nu}\Big(-\log(r)I + e_r e_r^T\Big),\quad \Pi(y) = \frac{y}{2\pi r^2}.$$

Theorem 3.3. *Guillaume and Hassine (2007); Hassine et al. (2008) Under the same hypotheses of theorem 3.2, the function j has the following asymptotic expansion*

$$j(\Omega\backslash\overline{\mathcal{O}_\varepsilon}) = j(\Omega) + \frac{-1}{\log(\varepsilon)}\,\delta j(x_0) + o\Big(\frac{-1}{\log(\varepsilon)}\Big).$$

where the topological gradient δj is given by

$$\delta j(x) = 4\pi\nu\, u_0(x)\cdot v_0(x) + \delta J(x),\ \ x\in\Omega.$$

3.3 Cost function examples

We now discuss Assumption 3.2. We present two standard examples of cost functions satisfying this Assumption and we calculate their variations δJ. For the proofs one can see Guillaume and Hassine (2007) or Hassine et al. (2008).

Proposition 3.2. *Let $w_d \in H^1(\Omega)$ be a given wanted (objective) velocity field. The cost function*

$$J_\varepsilon(u) = \int_{\Omega\backslash\overline{\mathcal{O}_\varepsilon}} |u - w_d|^2\,dx, \tag{13}$$

satisfies the assumption 3.1 with

$$DJ_0(w) = 2\int_\Omega (u_0 - w_d)\cdot w\,dx,\quad \forall w\in\mathcal{V}_0,\ \text{and}\ \delta J(x_0) = 0.$$

Proposition 3.3. *Let $w_d \in H^2(\Omega)$. The cost function*

$$J_\varepsilon(u) = \nu \int_{\Omega\setminus\overline{\mathcal{O}_\varepsilon}} |\nabla u - \nabla w_d|^2\, dx, \tag{14}$$

satisfies the assumption 3.1 with

$$DJ_0(w) = 2\int_\Omega \nabla(u_0 - w_d)\cdot\nabla w\, dx \quad \forall w \in \mathcal{V}_0,$$

$$\delta J(x_0) = \begin{cases} \left(-\int_{\partial\mathcal{O}} \eta(y)\, ds(y)\right)\cdot u_0(x_0) & \text{if } d = 3, \\ 4\pi\nu|u_0(x_0)|^2 & \text{if } d = 2. \end{cases}$$

For d=3, if $\mathcal{O}$ is the unit ball $B(0,1)$, we have $\delta J = 6\pi\nu|u_0(x_0)|^2$.

4. Numerical experiments

As an application of the previous theoretical results, we consider some engineering applications commonly found in the fluid mechanics literature. Our implementation is based on the following optimization algorithm.

4.1 The optimization algorithm

We apply an iterative process to build a sequence of geometries $(\Omega_k)_{k\geq 0}$ with $\Omega_0 = \Omega$. At the k^{th} iteration the topological gradient is denoted by δj_k and the new geometry Ω_{k+1} is obtained by inserting an obstacle $\mathcal{O}_k$ in the domain Ω_k; $\Omega_{k+1} = \Omega_k\setminus\overline{\mathcal{O}_k}$. The location and the size of the obstacle $\mathcal{O}_k$ are chosen in such a way that $j(\Omega_{k+1}) - j(\Omega_k)$ is negative.
Based on the last remark, the obstacle $\mathcal{O}_k$ is defined by a level set curve of the topological gradient δj_k

$$\mathcal{O}_k = \left\{x \in \Omega_k, \text{ such that } \delta j_k(x) \leq c_k \leq 0\right\},$$

where c_k is chosen in such a way that $|\mathcal{O}_k|/|\Omega_k|$ is less than a given ratio $\delta \in]0, 1[$.
The algorithm : Topology optimization with volume constraint.
• Initialization: choose $\Omega_0 = \Omega$, and set $k = 0$.
• Repeat until $|\Omega_k| \leq V_{desired}$:

- compute u_k the solution to the Stokes equations (15) in Ω_k,
- compute v_k the solution to the associated adjoint problem (16) in Ω_k ,
- compute the topological sensitivity $\delta j_k(z)$, $\forall z \in \Omega_k$,
- determine $\Omega_{k+1} = \Omega_k\setminus\overline{\mathcal{O}_k}$, where $\mathcal{O}_k = \left\{x \in \Omega_k, \text{ such that } \delta j_k(x) \leq c_k \leq 0\right\}$,
- $k \longleftarrow k+1$.

The topological gradient δj_k is defined by

$$\delta j_k(z) = u_k(z)\cdot v_k(z) + \delta J_k(z), \quad \forall z \in \Omega_k,$$

where u_k is the velocity field solution to

$$\begin{cases} -\nu\,\Delta u_k + \nabla p_k = F & \text{in } \Omega_k \\ \text{div } u_k = 0 & \text{in } \Omega_k, \end{cases} \tag{15}$$

and v_k is the solution to the associated adjoint problem

$$\begin{cases} -\nu\,\Delta v_k + \nabla q_k = -DJ(u_k) & \text{in } \Omega_k \\ \text{div } v_k = 0 & \text{in } \Omega_k. \end{cases} \tag{16}$$

The discretization of the problems (15) and (16) is based on the mixed finite element method $P1 + bubble/P1$ Arnold et al. (1984). The function δj_k is computed piecewise constant over elements. The term δJ_k is the variation of the considered cost function J (see Propositions 3.2 and 3.3). The constant c_k determines the volume of the obstacle $\mathcal{O}_k$ to be inserted. In practice, c_k is chosen in such a way that:

i- $\mathcal{O}_k \subset \left\{x \in \Omega_k, \text{ such that } \delta j_k(x) \leq 0\right\}$,

ii- the obstacle volume $|\mathcal{O}_k|$ is less or equal to 10% of the current domain volume $|\Omega_k|$ i.e. $|\mathcal{O}_k|/|\Omega_k| \leq 0.1$.

This algorithm can be seen as a descent method where the descent direction is determined by the topological sensitivity δj_k and the step length is given by the volume variation $|\Omega_k \backslash \Omega_{k+1}|$.

4.2 Pipes shape optimization

We consider a viscous and incompressible fluid in a tank Ω having one inlet Γ_{in} and some outlets Γ^i_{out}, $1 \leq i \leq m$. The aim is to determine the optimal design of the pipes that connects the inlet to the outlet of the domain minimizing the dissipated power in the fluid.

4.2.1 Comparison

In order to test the advantage of our approach, we compare our results to those obtained in Borrvall and Petersson (2003); Glowinski and Pironneau (1975). We consider two numerical examples in two dimensional (2D) case. The first one is the pipe bend example presented in Figure 1. This test case is treated by Borrvall and Petersson in Borrvall and Petersson (2003). The second one is the double pipe shown in Figure 2. It is also considered by Borrvall and Petersson in Borrvall and Petersson (2003) and recently by Guest and Prévost in Glowinski and Pironneau (1975). The aim here is to obtain the optimal shape minimizing the dissipated power in the fluid.

The considered design function is given by

$$j(D) = \nu \int_D |\nabla u_D|^2\, dx,$$

where u_D is the solution to the Stokes system in D.

The optimization problem consists in finding the fluid flow domain solution to

$$\min_{D \in \mathcal{D}_{ad}} j(D)\,,\ \text{such that } |D| \leq V_{desired}$$

where $\mathcal{D}_{ad}$ is the set of admissible domains defined by

$$\mathcal{D}_{ad} = \{D \subset \Omega \text{ such that } \Gamma_{in} \subset \partial\Omega \cap \partial D \text{ and } \Gamma^i_{out} \subset \partial\Omega \cap \partial D\}.$$

In both cases the inflow and the outflow conditions are given by a parabolic flow profile type with a maximum flow velocity equal to 1. Elsewhere the velocity is prescribed to be zero on the boundary of the domain.

A- Test 1 : *2D pipe bend example.* We consider a cavity $\Omega =]0,1[\times]0,1[$ having one inlet (left) and one outlet (bottom) (see figure 1(a)).

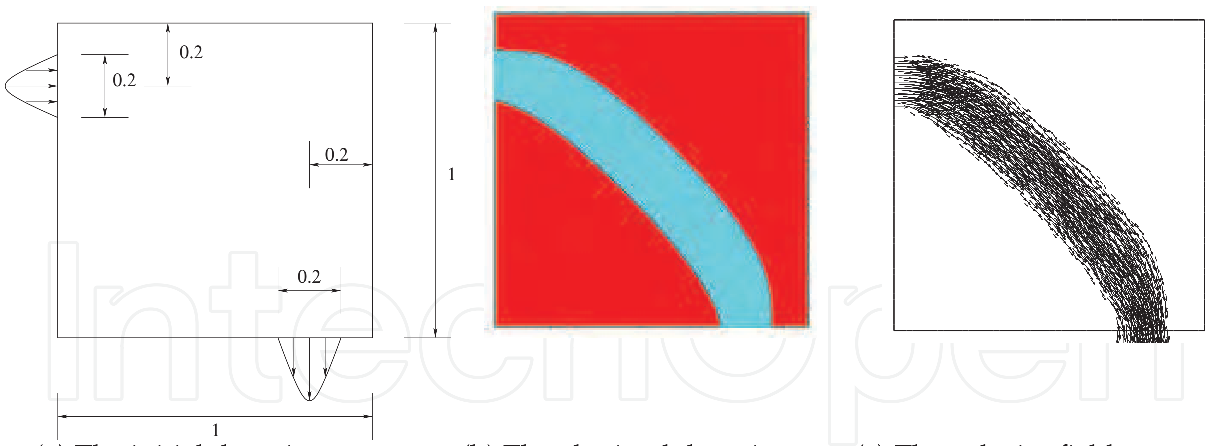

(a) The initial domain (b) The obtained domain (c) The velocity field

Fig. 1. 2D pipe bend example.

The cavity Ω is discretized using a finite elements mesh with 6561 nodes and 12800 triangular elements. The results of this example are presented in figure 1. The obtained pipe geometry is described in figure 1(b). It is computed using $V_{desired} = 0.08\pi\,|\Omega|$. The prescribed volume constraint is chosen so that the optimal solution has the same volume as a quarter torus of inner radius 0.7 and outer radius 0.9 that exactly fits to the inlet and outlet. In figure 1(c) we present the velocity field computed in the final domain.
The obtained solution is nearly identical to those presented in Borrvall and Petersson Borrvall and Petersson (2003). However, we obtain this result in 14 iterations, where Borrvall and Petersson needed more than sixty. As it can be seen, we have a more torus shaped pipe than in Borrvall and Petersson (2003), like most pipe bends in fluid mechanics literature. As it is stated in Glowinski and Pironneau (1975), the solution in Borrvall and Petersson Borrvall and Petersson (2003) contains regions of artificial material and does not sufficiently take into account the adherence condition.
B- Test 2: *2D double pipe example.* The initial domain of this example is shown in Figure 2(a). It is the rectangular $\Omega =]0, 3/2[\times]0, 1[$ with two inlets and two outlets.

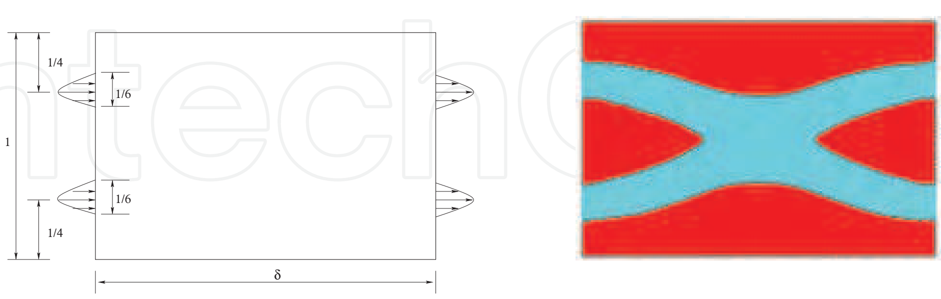

(a) The initial domain (b) The obtained domain

Fig. 2. The initial and the optimal domains for the 2D double pipe example.

The cavity Ω is discretized using a finite elements mesh with 9801 nodes and 19200 triangular elements. The results of this example are presented in figure 2. The final geometry is computed with $V_{desired} = \dfrac{1}{3}\,|\Omega|$.

We present in figure 2(b) the obtained geometry. The final geometry is obtained in only 12 iterations, where Borrvall and Petersson needed more than sixty. We remark that the two pipes join to form a single, wider pipe through the center of the domain. This design decreases the length of the fluid-solid interface by decreasing the power lost. As it can be seen, the optimal solution is identical to that obtained by Guest and Prévost Glowinski and Pironneau (1975), but it does not match that of Borrvall and Petersson Borrvall and Petersson (2003). As for the pipe bend example, the solution in Borrvall and Petersson (2003) contains regions of artificial material and does not sufficiently take into account the adherence condition.

4.2.2 Three dimensional case

In this section we propose an extension of the two 2D examples considered in the last section to the three dimensional case.

A- Example 1 : *3D pipe bend example.* For the 3D pipe bend example, the initial domain is the unit cube $\Omega =]0,1[\times]0,1[\times]0,1[$ having one inlet and one outlet (see figure 3). The inlet Γ_{in} (left) and the outlet Γ_{out} (bottom) are described by the following discs

$$\Gamma_{in} = B(z_{in}, 0.1) \cap \{0\}\times]0,1[\times]0,1[, \text{ and } \Gamma_{out} = B(z_{out}, 0.1)\cap]0,1[\times]0,1[\times\{0\},$$

where $B(z_\beta, 0.1)$, $\beta = in, out$, is the ball of center z and radius 0.1, with $z_{in} = (0, 0.5, 0.8)$ and $z_{out} = (0.8, 0.5, 0)$.

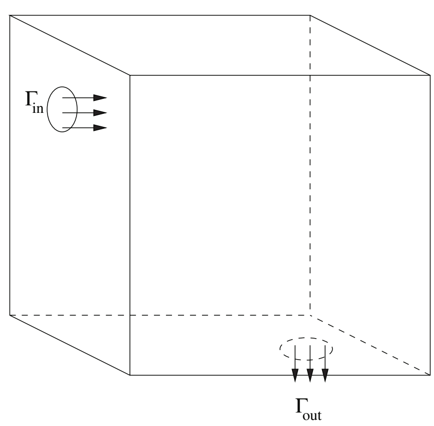

Fig. 3. The initial domain

For the boundary conditions, we consider a parabolic flow profile type with a maximum flow velocity equal to 1 on Γ_{in} and Γ_{out}, and a velocity equal to zero elsewhere. The domain is discretized using 29791 nodes and 162000 tetrahedral elements.
Like in the 2D case, we aim to determine the optimal design of the pipe that connects the inlet to the outlet of the domain and minimizes the dissipated power in the fluid. We present in figure 4 the optimal pipe domains obtained for different volume constraint $V_{desired}$ choices. The first case (figure 4(a)), corresponding to $V_{desired} = 0.50\,|\Omega|$, is obtained after 7 iterations, the second one (figure 4(b)) after 11 iterations for $V_{desired} = 0.35\,|\Omega|$ and the last one (figure 4(b)) needs 16 iterations to reach $V_{desired} = 0.20\,|\Omega|$. We show in figure 5 a 2D cut of the velocity field corresponding to the three obtained domains.

B- Example 2 : *3D double pipe bend example.* The initial domain is the cavity $\Omega =]0,3/2[\times]0,1[\times]0,1[$ (described in figure 6). It has two inlets (left) Γ^i_{in}, i=1,2, and two outlets

(a) $V_{desired} = 0.50\,|\Omega|$. (b) $V_{desired} = 0.35\,|\Omega|$. (c) $V_{desired} = 0.20\,|\Omega|$.

Fig. 4. The obtained domains (see Abdelwahed, Hassine and Masmoudi (2009)).

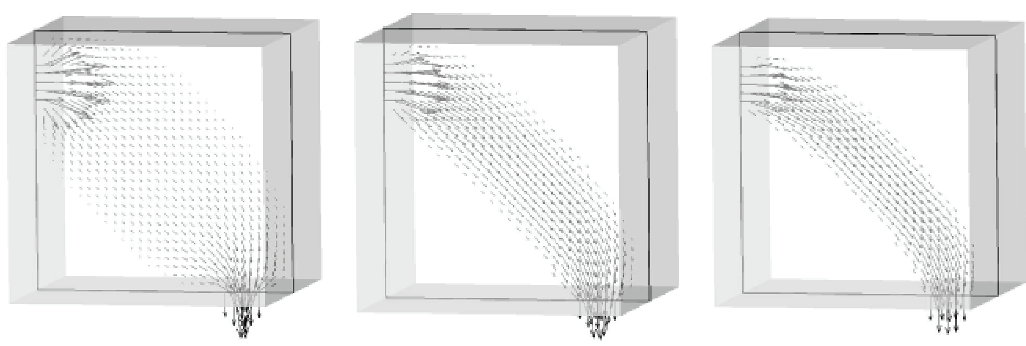

Case (a) Case (b) Case (c)

Fig. 5. 2D vertical cut of the velocity field in the obtained domains.

(right) Γ^i_{out}, i=1,2 defined by

$$\Gamma^1_{in} = B(z^1_{in}, 0.1) \cap \{0\}\times]0,1[\times]0,1[,\ \Gamma^2_{in} = B(z^2_{in}, 0.1) \cap \{0\}\times]0,1[\times]0,1[,$$
$$\Gamma^1_{out} = B(z^1_{out}, 0.1) \cap \{3/2\}\times]0,1[\times]0,1[,\ \Gamma^2_{out} = B(z^2_{out}, 0.1) \cap \{3/2\}\times]0,1[\times]0,1[,$$

where

$$z^1_{in} = (0, 1/2, 1/4),\ z^2_{in} = (0, 1/2, 3/4),\ z^1_{out} = (3/2, 1/2, 1/4), \text{ and } z^2_{out} = (3/2, 1/2, 3/4)$$

For the boundary conditions, as in the last example, we consider a parabolic flow profile type with a maximum flow velocity equal to 1 on Γ^i_{in} and on Γ^i_{out}, and a velocity equal to zero elsewhere. We use a mesh with 160602 nodes and 895900 tetrahedral elements.
We present in figure 7 the optimal shape design obtained respectively for $V_{desired} = 0.40\,|\Omega|$ (9 iterations) and $V_{desired} = 0.10\,|\Omega|$ (21 iterations). A vertical cut of the corresponding velocity field is shown in figure 8.

4.2.3 Shape optimization of tubes in a 3D cavity

In this section we treat the shape optimization of tubes in a cavity. We consider an incompressible fluid in a cavity Ω having one inlet Γ_{in} and four outlets Γ^i_{out}, $i = 1, 4$. The aim here is to determine the optimal shape of the tubes that connect the inlet to the outlets of the cavity maximizing the outflow rate. It consists in inserting small obstacles in the cavity in order to maximize the outflow rate at Γ^i_{out}, $i = 1, 4$.

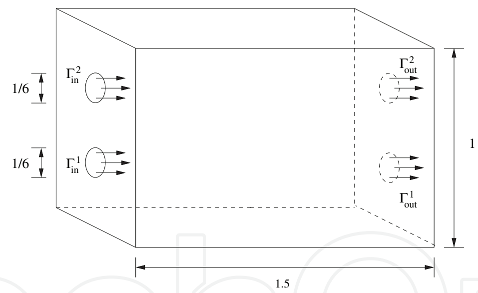

Fig. 6. The initial domain

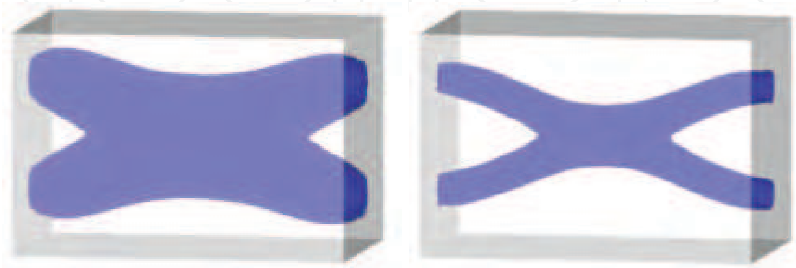

(a) $V_{desired} = 0.40\,|\Omega|$. (b) $V_{desired} = 0.10\,|\Omega|$.

Fig. 7. The optimal domains (see Abdelwahed, Hassine and Masmoudi (2009)).

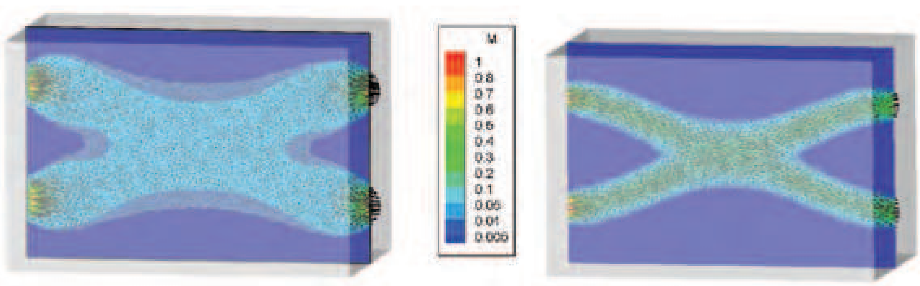

Fig. 8. 2D vertical cut of the velocity isovalues and field in the optimal domains.

In our numerical computation, we have used the cavity $\Omega =]0,1[\times]0,1[\times]0,1[$ with the inlet Γ_{in}:
$\Gamma_{in} = \left\{(x,y,z) \in \Omega \text{ such that } x^2 + (y-0.5)^2 + (z-0.5)^2 \leq 0.04\right\}$
and the four outlets Γ^1_{out}, Γ^2_{out}, Γ^3_{out} and Γ^4_{out}:

$$\Gamma^1_{out} = \left\{(x,y,z) \in \Omega \text{ such that } (x-0.75)^2 + (y-0.5)^2 + z^2 \leq 0.0025\right\},$$

$$\Gamma^2_{out} = \left\{(x,y,z) \in \Omega \text{ such that } (x-0.75)^2 + (y-0.5)^2 + (z-1)^2 \leq 0.0025\right\},$$

$$\Gamma^3_{out} = \left\{(x,y,z) \in \Omega \text{ such that } (x-0.75)^2 + y^2 + (z-0.5)^2 \leq 0.0025\right\},$$

$$\Gamma^4_{out} = \left\{(x,y,z) \in \Omega \text{ such that } (x-0.75)^2 + (y-1)^2 + (z-0.5)^2 \leq 0.0025\right\}.$$

The considered cost function measuring the outflow rate is given by

$$j(D) = \sum_{i=1}^{m} \int_{\Gamma^i_{out}} |u_D.\mathbf{n}| \text{ ds},$$

where $D \in \mathcal{D}_{ad}$ and u_D is the velocity field, solution to the Stokes equations in D satisfying the following boundary conditions :

- A free surface boundary condition on the outlets

$$\sigma(u) \cdot \mathbf{n} = 0 \text{ on } \cup_{i=1}^{m} \Gamma_{out}^{i},$$

  where $\sigma(u) = \nu(\nabla u + \nabla u^T) - pI$, I is the 3×3 identity matrix and $\mathbf{n}$ denotes the outward normal to the boundary.

- The normal component of the stress tensor is prescribed on the inlet Γ_{in}

$$\sigma(u) \cdot \mathbf{n} = g \text{ on } \Gamma_{in},$$

- The velocity is equal to zero on $\Gamma \backslash (\cup_{i=1}^{m} \Gamma_{out}^{i} \cup \Gamma_{in})$.

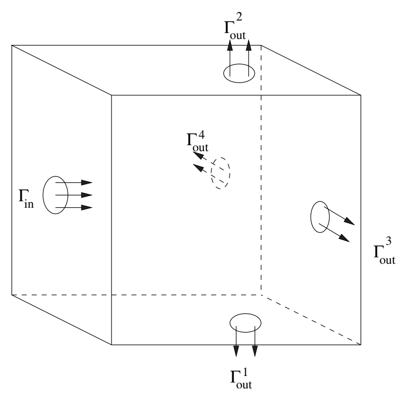

Fig. 9. The initial domain.

The results of this example are described in figures 10-13. In figure 10 we present the obtained geometries for different volume constraints. We present the obtained geometry: in figure10(a) for $V_{desired} = 0.35\,|\Omega|$, in figure10(b) for $V_{desired} = 0.25\,|\Omega|$ and in figure10(b) for $V_{desired} = 0.15\,|\Omega|$. This domains are obtained respectively after 10, 14 and 19 iterations. The associated velocities fields are given in figures 11 and 12. In figure 13 we illustrate the variation of the outflow rate.

(a) $V_{desired} = 0.35\,|\Omega|$. (b) $V_{desired} = 0.25\,|\Omega|$. (c) $V_{desired} = 0.15\,|\Omega|$.

Fig. 10. The optimal domains (see Abdelwahed, Hassine and Masmoudi (2009)).

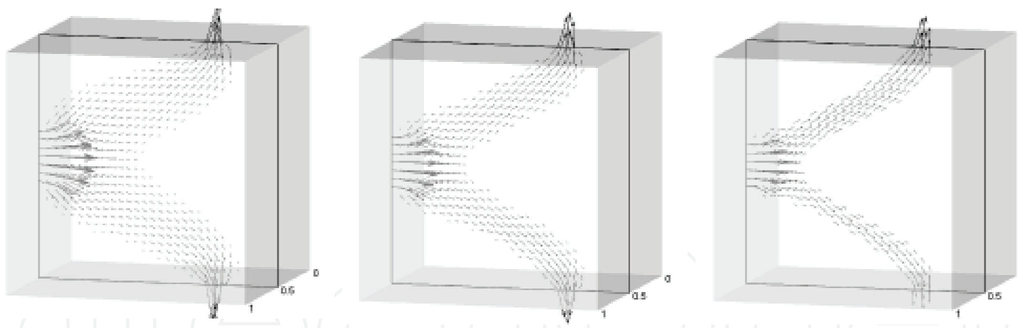

Case (a) Case (b) Case (c)

Fig. 11. 2D vertical cut of the velocity field.

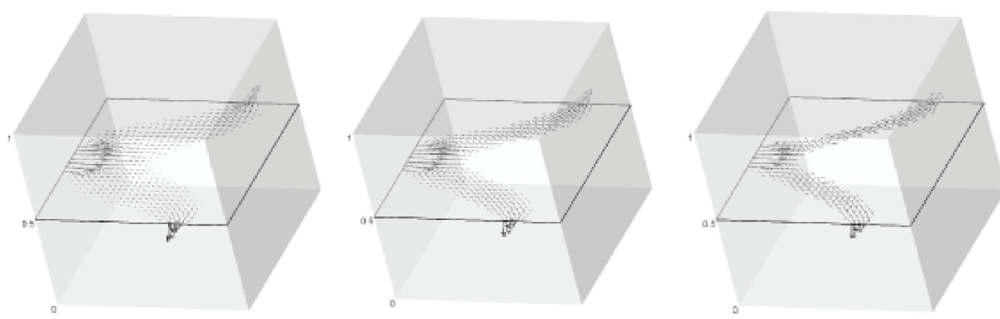

(a) (b) (c)

Fig. 12. 2D horizontal cut of the velocity field.

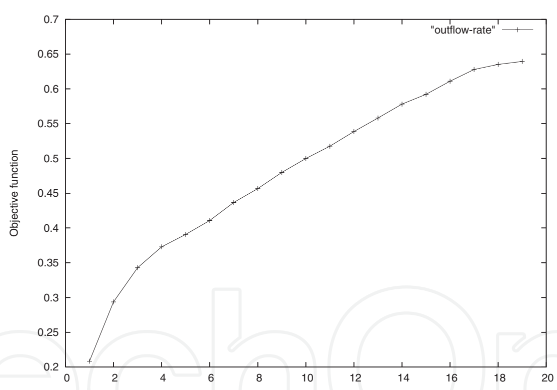

Fig. 13. Variation of the outflow rate

4.3 Optimization of injectors location in an eutrophic lake

Eutrophication is a complex phenomena involving many physico-chemical parameters. Specifically in some climatic areas, the thermic factors combined to the biological and to the biochemical ones are dominant in the behavior of the aquatic ecosystems. Consequently, they generate important bio-climatology variations creating in lakes an unsteady dynamic process that decreases progressively water quality. Practically, the eutrophication in a water basin is characterized mainly by a poor dissolved oxygen concentration in water. Furthermore, this phenomena is accompanied by a stratification process dividing the water volume, during a large period of the year, into three distinct layers as depicted in Figure 14.
Three zones constitute this stratification:

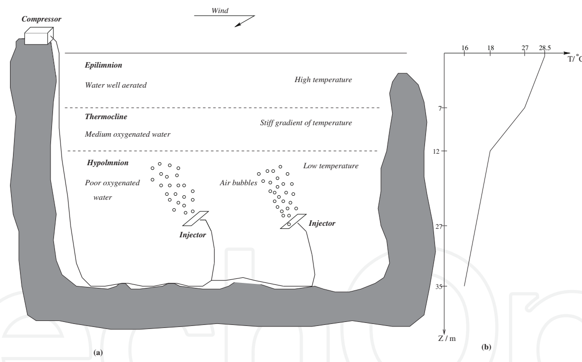

Fig. 14. (a): Structure of a stratified lake, (b): average temperature curve during summer

i) at the top, the epilimnion, a layer of around 7 m depth, well mixed by the effect of drafting wind and consequently well aerated,

ii) in the middle, the thermocline, a zone with a quick decrease of temperature (27 ^{o}C to 18 ^{o}C) and of 5 m depth. This area is weakly affected by the wind action and consequently a medium concentration of oxygen is observed,

iii) at the bottom, the hypolimnion, a deeper layer beyond 12 m, having a temperature varying from 18 ^{o}C to 14 ^{o}C. This region is characterized by a low concentration of oxygen and a high concentration of toxic gas (H_2S, ammoniac, carbonic gas, etc.)

The dynamic aeration process seems to be the most promising remedial technique to treat water eutrophication. This technique consists in inserting air by the means of injectors located at the bottom of the lake in order to generate a vertical motion mixing up the water of the bottom with that in the top, thus oxygenating the lower part by bringing it in contact with the surface air.

Theoretically, the bubble flow is a multi-phase flow where the presence of free interfaces raises difficulties in both the physical and mathematical modelling. Hence, to obtain a physical and significant resolution by numerical simulation of the air injection phenomena in an eutrophised lake, one should consider a two-phase model: water-air bubble (see Ishii Ishii (1975)). This kind of modelling involves large systems of PDE's and variables in a multi-scale frame as well as closure conditions through turbulence model and phases interface interaction. Moreover, the domain mesh size should be "small" in order to capture the significant variations of the spectrum. Therefore, the computational cost should be also addressed.

For all these reasons, we consider here, as a first approximation, only the liquid phase, which is the dominant one. The flow is described by a simplified model based on incompressible Stokes equations. The injected air is taken into account through local boundary conditions for the velocity on the injectors holes. In order to generate the best motion in the fluid with respect to the aeration purpose, the topological sensitivity analysis method is used to optimize the injectors location.

4.3.1 Optimization problem

In this section, we use the topological sensitivity analysis method to optimize the injector locations in the lake Ω in order to generate the best motion in the fluid with respect to the aeration purpose.

To this end, each injector Inj_k is modeled as a small hole $\mathcal{B}_{z_k,\varepsilon} = z_k + \varepsilon\mathcal{B}^k$, $1 \leq k \leq m$ having an injection velocity u^k_{inj}, where ε is the shared diameter and $\mathcal{B}^k \subset \mathbb{R}^d$ are bounded and

smooth domains containing the origin. The points $z_k \in \Omega,\ 1 \leq k \leq m$ determine the location of the injectors.
Then, in the presence of injectors, the velocity u_ε and the pressure p_ε satisfy the following system

$$\begin{cases} -\nu\Delta u_\varepsilon + \nabla p_\varepsilon = F & \text{in } \Omega\backslash\cup_{k=1}^{m}\overline{\mathcal{B}_{z_k,\varepsilon}} \\ \text{div } u_\varepsilon = 0 & \text{in } \Omega\backslash\cup_{k=1}^{m}\overline{\mathcal{B}_{z_k,\varepsilon}} \\ u_\varepsilon = u_d & \text{on } \Gamma \\ u_\varepsilon = u_{inj}^k & \text{on } \cup_{k=1}^{m}\partial\mathcal{B}_{z_k,\varepsilon}, \end{cases} \tag{17}$$

where u_{inj}^k is a given injection velocity on $\partial\mathcal{B}_{z_k,\varepsilon},\ 1 \leq k \leq m$.

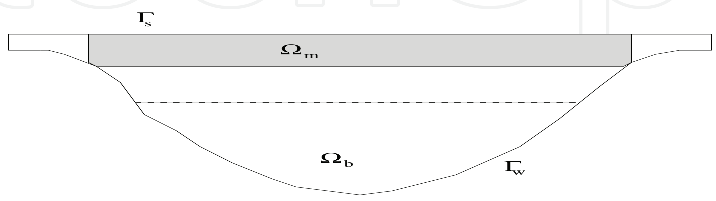

Fig. 15. The geometry of the lake.

Concerning the optimization criteria, we assume that a "good" lake oxygenation can be described by a target velocity $\mathcal{U}_g$. Then, the cost function J_ε to be minimized is defined by

$$J_\varepsilon(u_\varepsilon) = \int_{\Omega_m} |u_\varepsilon - \mathcal{U}_g|^2\, dx, \tag{18}$$

where $\Omega_m \subset \Omega$ is the measurement domain (the top layer, see Figure 15).
Consider the design function j of the form

$$j(\Omega\backslash \cup_{k=1}^{m} \overline{\mathcal{B}_{z_k,\varepsilon}}) = J_\varepsilon(u_\varepsilon), \tag{19}$$

Our identification problem can be formulated as a topological optimization problem one. It consists in finding the optimal location of the holes $\mathcal{B}_{z_k,\varepsilon} = z_k + \varepsilon\mathcal{B}^k,\ 1 \leq k \leq m$, inside the domain Ω in order to minimize the optimal design function j.

$$(\mathcal{O}_\varepsilon) \begin{cases} \text{Find } z_k^* \in \Omega,\ 1 \leq k \leq m, \text{ such that :} \\ j(\Omega\backslash \cup_{k=1}^{m} \overline{\mathcal{B}_{z_k^*,\varepsilon}}) = \min\limits_{\mathcal{B}_{z_k,\varepsilon}\subset\Omega} j(\Omega\backslash \cup_{k=1}^{m} \overline{\mathcal{B}_{z_k,\varepsilon}}). \end{cases}$$

To solve this optimization problem $(\mathcal{O}_\varepsilon)$ we have used the topological sensitivity analysis method. It consists in studying the variation of the design function j with respect to the presence of a small injector $\mathcal{B}_{z,\varepsilon} = z + \varepsilon\mathcal{B}$ in the lake Ω.

4.3.2 Numerical results

We propose an adaptation of the previous algorithm to our context. At the k^{th} iteration, the topological gradient δj_k is given by

$$\delta j_k(z) = \Big(u_k(x) - u_{inj}\Big) \cdot v_k(x), \quad \forall z \in \Omega_k \tag{20}$$

where u_k and v_k are, respectively, solutions to the direct and adjoint problems in Ω_k.
We consider the set $\{x \in \Omega_k; \quad \delta j_k(x) < c_{k+1}\}$. Each connected component of this set is a hole created by the algorithm. Our idea is to replace each hole by an injector located at the local minimum of $\delta j_k(x)$. The obtained results are described in figures 16 and 17.

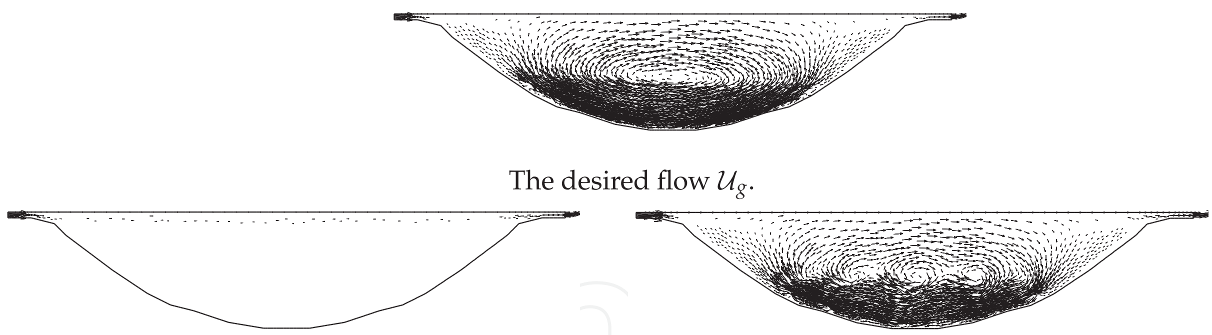

The desired flow $\mathcal{U}_g$.

The initial velocity field

The obtained velocity field

Fig. 16. Numerical results in 2D (for more details one can see Hassine and Masmoudi (2004)).

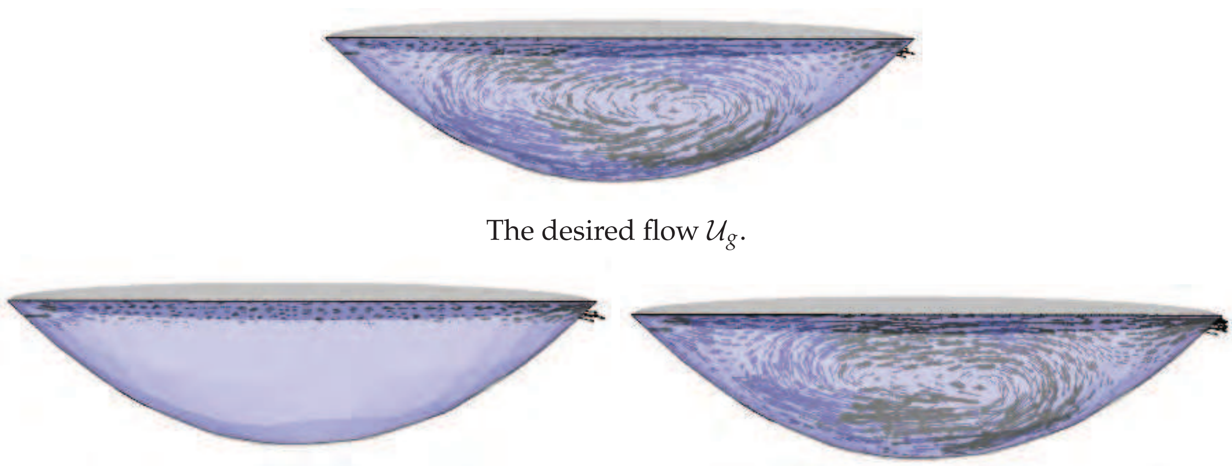

The desired flow $\mathcal{U}_g$.

The initial velocity field.

The obtained velocity field

Fig. 17. Numerical results in 3D (see Abdelwahed, Hassine and Masmoudi (2009)).

4.4 Geometrical control of fluid flow

We consider a tank Ω filled with a viscous and incompressible fluid. The aim is to determine the optimal shape of the fluid flow domain minimizing a given objective function.

4.4.1 Approximation of a desired flow

The aim is to determine the optimal shape $\mathcal{O}^* \subset \Omega$ of the fluid flow domain such that the velocity $u_{\mathcal{O}^*}$, solution to the Stokes equations in $\mathcal{O}^*$, approximate a desired flow w_d defined in a fixed domain Ω_m. The optimal shape $\mathcal{O}^*$ can be characterized as the solution to the following topological optimization problem

$$\min_{D\subset\Omega} \int_{\Omega_m} |u_D - w_d|^2 dx,$$

where u_D is the solution to the Stokes equations in $D \subset \Omega$. This test is treated in two and three dimensional cases. In 2D, the tank $\Omega = [0, 1.5] \times [0, 1]$, the domain $\Omega_m = [0, 1.5] \times [0.8, 1]$ and the velocity field w_d is defined by

$$w_d = \begin{cases} (1, 0) \text{ in } \Omega_m, \\ (0, 0) \text{ elsewhere} . \end{cases}$$

The numerical results are described in Figure 18. A 3D extension of this case is presented in Figure 19.

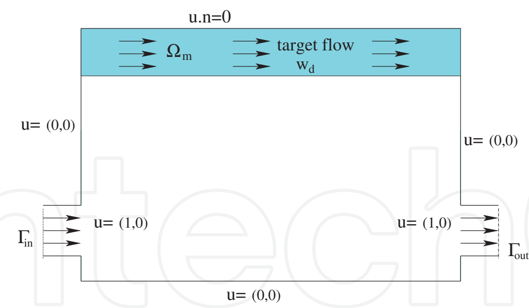

(a) The initial geometry Ω

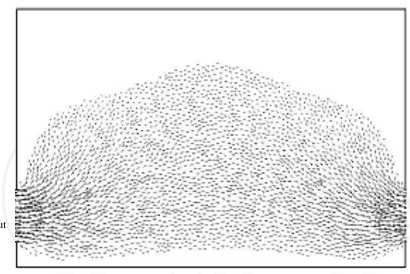

(b) The velocity field in the initial domain

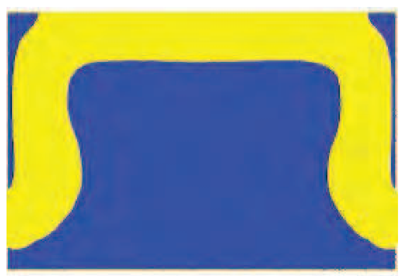

(c) The optimal domain is obtained in only 3 iterations

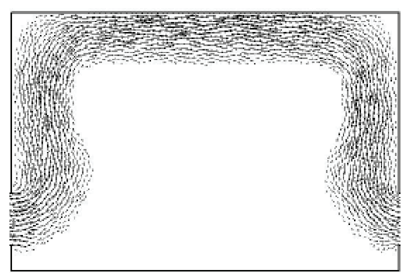

(d) The velocity field in the obtained domain

Fig. 18. Approximation of a desired flow: 2D case

4.4.2 Maximizing velocity in a fixed zone

Here the aim is to maximize the fluid flow velocity in $\Omega_m = \cup_k \Omega_m^k \subset \Omega$ (fixed zones) using a topological perturbation of the domain. The optimal domain of the fluid flow can be characterized as a solution to the following problem

$$\max_{\mathcal{O}\subset\Omega} \int_{\Omega_m} |u_{\mathcal{O}}|^2 \mathrm{dx},$$

where $u_{\mathcal{O}}$ is the solution to the Stokes equations in $\mathcal{O}$.
Two 3D test cases are considered. The first case is described in Figure 20. The inflow Γ_{in} and the outflow Γ_{out} (see Figure 20(a)) are defined by
$\Gamma_{in} = [0, 1.5] \times 0 \times [0.4, 0.6]$, $\Gamma_{out} = [0, 1.5] \times 0 \times [0.4, 0.6]$.
The domain $\Omega_m = \Omega_m^1 \cup \Omega_m^2$, with $\Omega_m^1 = [0, 1.5] \times [0, 1] \times [0.9, 1]$ and $\Omega_m^2 = [0, 1.5] \times [0, 1] \times [0, 0.1]$.
The optimal domain (see Figure 20(c)) is obtained in four iterations.
The second case is described in Figure 21. Here we have used the same 3D tank considered in the last case but with different Γ_{in}, Γ_{out} and Ω_m (see Figure 21(a)). The optimal domain (see Figure 21(c)) is obtained in five iterations.

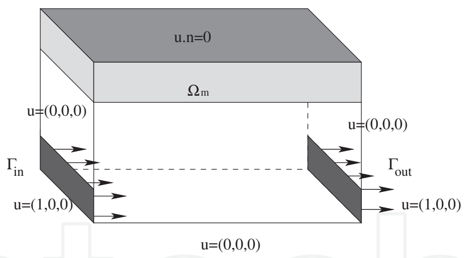

(a) The initial geometry

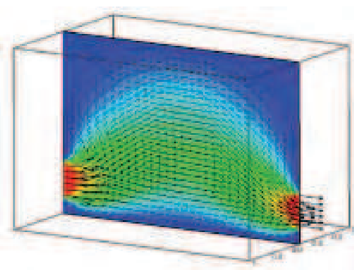

(b) The velocity field in the initial domain

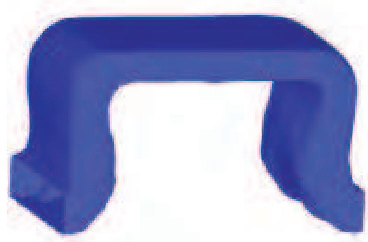

(c) The optimal domain is obtained in only 4 iterations

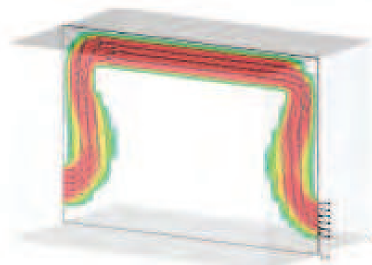

(d) The velocity field in the obtained domain

Fig. 19. Approximation of a desired flow: 3D case

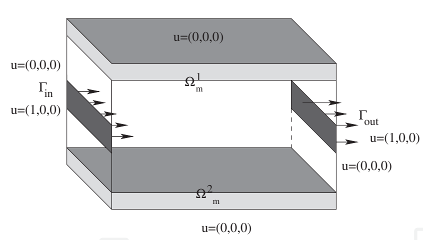

(a) The initial geometry

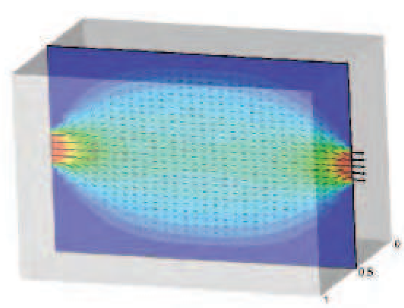

(b) Cut of the initial velocity

(c) The optimal domain

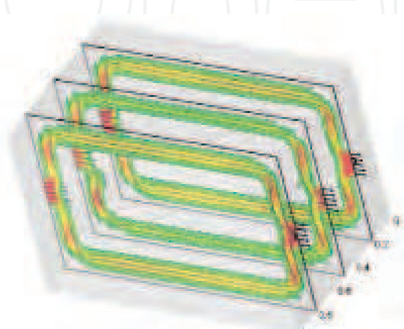

(d) 2D cuts of the optimal velocity

Fig. 20. Maximizing velocity in a fixed zone: first case (see Abdelwahed and Hassine (2009))

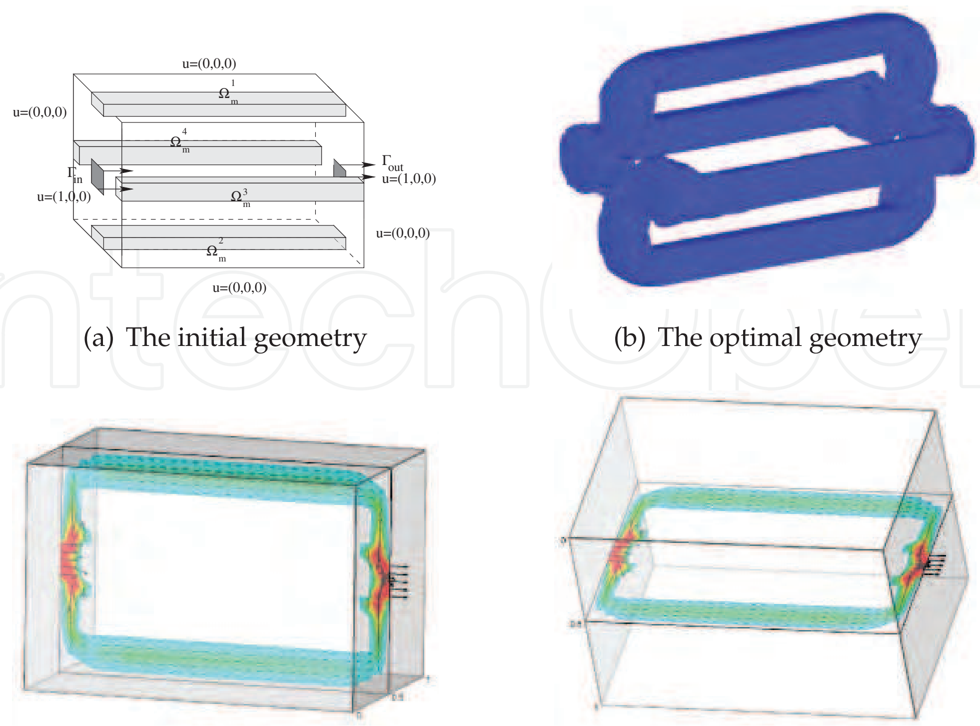

(a) The initial geometry

(b) The optimal geometry

(c) Vertical cut of the velocity in the obtained domain

(d) Horizontal cut of velocity in the obtained domain

Fig. 21. Maximizing velocity in a fixed zone: second case (see Abdelwahed and Hassine (2009))

5. Conclusion

In this chapter we have proposed an accurate and fast topological optimization algorithm. The optimal domain is obtained iteratively by inserting some obstacles at each iteration. The location and size of the obstacles are described by a scalar function called the topological gradient. The topological gradient is derived as the leading term of the cost function variation with respect to the insertion of a small obstacle in the fluid flow domain.
The proposed method has two main features. The first one concerns its mathematical framework. The topological sensitivity analysis can be adapted for various operators like elasticity, Helmholtz, Maxwell, Navier Stokes, ...
The second interesting feature of the approach is that it leads to a fast and accurate numerical algorithm. Only a few iterations are needed to construct the final domain. It is easy to be implemented and can be used for many applications. At each iteration we only need to solve the direct and the adjoint problems on a fixed grid.

6. References

M. Abdelwahed and M. Hassine, *Topological optimization method for a geometric control problem in Stokes flow*, Journal of Applied Numerical Mathematics, Volume 59 (8), 2009, 1823-1838.

M. Abdelwahed, M. Hassine and M. Masmoudi, *Optimal shape design for fluid flow using topological perturbation technique*, Journal of Mathematical Analysis and Applications, Volume 356, 2009, 548–563.

M. Abdelwahed, M. Hassine and M. Masmoudi, *Control of a mechanical aeration process via topological sensitivity analysis*, Journal of Computational and Applied Mathematics, Volume 228 (1), 2009, 480–485.

G. Allaire and R. Kohn, *Optimal bounds on the effective behavior of a mixture of two well-orded elastic materials*, Quartely of Applied Mathematics, Li(4), 1996, 643-674.

A. Ben Abda, M. Hassine, M. Jaoua, M. Masmoudi, *Topological sensitivity analysis for the location of small cavities in Stokes flow*, SIAM J. Contr. Optim. Vol. 48 (5), 2009, 2871–2900

S. Amstutz, *The topological asymptotic for Navier Stokes equations*, ESAIM, Cont. Optim. Cal. Var. 11 (3), 2005, 401-425.

S. Amstutz, M. Masmoudi and B. Samet, *The topological asymptotic for the Helmholtz equation*, SIAM J. Contr. Optim, 42 (2003), 1523-1544.

D. Arnold, F. Brezzi and M. Fortin (1984), *A stable finite element for the Stokes equations*, Calcolo, 21 (4) (1984), 337-344.

M. Bendsoe, *Optimal topology design of continuum structure: an introduction*. Technical report, Departement of mathematics, Technical University of Denmark, DK2800 Lyngby, Denmark, september 1996.

T. Borrvall and J. Petersson, *Topological optimization of fluids in Stokes flow*, Inter. J. Numer. Methods Fluids, 41 (1), 2003, 77-107.

G. Buttazzo and G. Dal Maso, *Shape optimization for Dirichlet problems: Relaxed formulation and optimality conditions*, Appl. Math. Optim. 23 (1991), 17-49.

H. Cabuk and V. Modi, *Optimum plane diffusers in laminar flow*, J. of Fluid Mechanics 237 (1992), 373-393.

J. Céa, S. Garreau, Ph. Guillaume and M. Masmoudi, *The shape and Topological Optimizations Connection*, Comput. Methods Appl. Mech. Engrg. 188(4), (2000) 713-726.

E.M. Cliff, M. Heinkenschloss and A. Shenoy, *Airfoil design by an all-at-once method*, Inter. J. Compu. Fluid Mechanics 11 (1998) 3-25.

S.S. Collis, K. Ghayour, M. Heinkenschloss, M. Ulbrich and S. Ulbrich, *Optimal control for unsteady compressible viscous flows*, Inter. J. Numer. Meth. Fluids 40 (2002) 1401-1429.

R. Dautray and J. Lions, *Analyse mathémathique et calcul numérique pour les sciences et les techniques*, MASSON, collection CEA, 1987.

A. Evgrafov, *The Limits of Porous Materials in the Topology Optimization of Stokes Flows*, Applied Mathematics and Optimization 52 (3), (2005) 263-277.

S. Garreau, Ph. Guillaume and M. Masmoudi, *The topological asymptotic for pde systems: the elasticity case*, SIAM J. Control Optim., 39(4) (2001) 1756-1778.

D.K. Gartling, C.E.Hickox and R.C. Givler, *Simulation of coupled viscous and porous flow problems*, Comp. Fluid. Dyn., 7(1) (1996) 23-48.

O. Ghattas and J-H. Bark, *Optimal control of two and three dimensional incompressible Navier-Stokes flows*, Journal of Computational Physics, 136 (1997) 231-244.

R. Glowinski and O. Pironneau, *On the numerical computation of the minimum drag profile in laminar flow*, J. of Fluid Mechanics 72 (1975) 385-389.

J. K. Guest and J. H. Prévost, *Topology optimization of creeping fluid flows using a Darcy-Stokes finite element*, Inter. J. Numer. Methods in Engineering 66 (2006) 461-484.

Ph. Guillaume and M. Hassine, *Removing holes in topological shape optimization*, ESAIM, COCV J. vol. 14 (1) (2007) 160-191.

Ph. Guillaume and K. Sid Idris, *Topological sensitivity and shape optimization for the Stokes equations*. SIAM J. Control Optim. 43(1) (2004) 1-31.

M.D. Gunzburger *Perspectives in flow control and optimization*, Advances in Design and Control, SIAM, Philadelphia, PA, 2003.

M.D. Gunzburger, L. Hou and T. Sovobodny, *Analysis and finite element approximation of optimal control problems for the stationary Navier-Stokes equations with Dirichlet controls*, RAIRO Model. Math. Anal. Numer. 25 (1991) 711-748.

M. Gunzburger, H. Kim and S. Manservisi, *On a shape control problem for the stationary Navier-Stokes equations*, M2AN Math. Model. Numer. Anal. 34 (6) (2000) 1233-1258.

M. Hassine, *Shape optimization for the Stokes equations using topological sensitivity analysis*, ARIMA Journal, vol. 5, (2006) 213-226.

M. Hassine, *Topological Sensitivity Analysis: theory and applications*, Habilitation Universitaire, El Manar University, Tunisia, 2008.

M. Hassine, S. Jan and M. Masmoudi, *From differential calculus to* $0-1$ *topological optimization*, SIAM J. Cont. Optim. vol.45 (6) (2007) 1965-1987.

M. Hassine and M. Masmoudi, *The topological asymptotic expansion for the Quasi-Stokes problem*, ESAIM, COCV J. vol. 10 (4) (2004) 478-504.

M. Ishii, *Thermo-fluid dynamic theory of a two-phase flow*, Collection de la direction des études de recherche d'électricité de france, EYROLLES, 1975.

D.W. Kim and M.U. Kim, *Minimum drag shape in two two-dimensional viscous flow*, Inter. J. Numer. Methods in Fluids 21 (1995) 93-111.

E. Lund, H. Moller and L.A. Jakobsen, *Shape Optimization of Fluid-Structure Interaction Problems Using Two-Equation Turbulence Models*. In Proc. 43rd Structures, Structural Dynamics, and Materials Conference and Exhibit, 2002, Denver, Colorado (CDROM), AIAA 2002-1478, 11 pages.

M. Masmoudi, *The topological asymptotic*, In Computational Methods for Control Applications, ed. H. Kawarada and J. Periaux, International Séries GAKUTO, 2002.

B. Mohammadi and O. Pironneau, *Applied shape optimization for fluids*, Numerical Mathematics and Scientific Computation, Oxford University Press, New York, 2001.

O. Pironneau, *On the transport-diffusion algorithm and its applications to the Navier-Stokes equations*, Numerische Mathematik, 38 (1982), 309-332.

O. Pironneau, *On optimum profiles in Stokes flow*, J. of Fluid Mechanics 59 (1973) 117-128.

O. Pironneau, *On optimum design in fluid mechanics*, J. of Fluid Mechanics 64 (1974) 97-110.

O. Pironneau, *Optimal Shape Design for Elliptic Systems*, Springer, Berlin (1984).

J. Simon, *Domain variation for drag Stokes flows*. In Lecture Notes in Control and Inform. Sci. 114, A. Bermudez Eds. Springer, Berlin (1987) 277-283.

A. Schumacher, *Topologieoptimierung von bauteilstrukturen unter verwendung von lopchpositionierungkrieterien*, thesis, Universitat-Gesamthochschule-Siegen, 1995.

J. Sokolowski and A. Zochowski, *On the topological derivative in shape optimization*, SIAM J. Control Optim., 37 (4) (1999) 1251-1272.

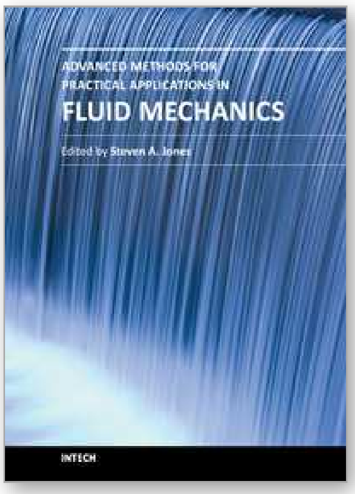

Advanced Methods for Practical Applications in Fluid Mechanics
Edited by Prof. Steven Jones

ISBN 978-953-51-0241-0
Hard cover, 230 pages
Publisher InTech
Published online 14, March, 2012
Published in print edition March, 2012

Whereas the field of Fluid Mechanics can be described as complicated, mathematically challenging, and esoteric, it is also imminently practical. It is central to a wide variety of issues that are important not only technologically, but also sociologically. This book highlights a cross-section of methods in Fluid Mechanics, each of which illustrates novel ideas of the researchers and relates to one or more issues of high interest during the early 21st century. The challenges include multiphase flows, compressibility, nonlinear dynamics, flow instability, changing solid-fluid boundaries, and fluids with solid-like properties. The applications relate problems such as weather and climate prediction, air quality, fuel efficiency, wind or wave energy harvesting, landslides, erosion, noise abatement, and health care.